US Army Corps of Engineers

AD-A216 113

TECHNICAL REPORT HL-89-22

AN ANALYSIS OF TRAINING STRUCTURE DESIGNS IN SOUTHWEST PASS, MISSISSIPPI RIVER

by

S. B. Heltzel, W. D. Martin, R. C. Berger, D. R. Richards

Hydraulics Laboratory

DEPARTMENT OF THE ARMY
Waterways Experiment Station, Corps of Engineers
3909 Halls Ferry Road, Vicksburg, Mississippi 39180-6199

November 1989

Final Report

Prepared for US Army Engineer District, New Orleans
New Orleans, Louisiana 70160-0267

HYDRAULICS LABORATORY

Unclassified

SECURITY CLASSIFICATION OF THIS PAGE

REPORT DOCUMENTATION PAGE

Form Approved OMB No. 0704-0188

1a. REPORT SECURITY CLASSIFICATION Unclassified	1b. RESTRICTIVE MARKINGS
2a. SECURITY CLASSIFICATION AUTHORITY	3. DISTRIBUTION/AVAILABILITY OF REPORT Approved for public release; distribution unlimited.
2b. DECLASSIFICATION/DOWNGRADING SCHEDULE	
4. PERFORMING ORGANIZATION REPORT NUMBER(S) Technical Report HL-89-22	5. MONITORING ORGANIZATION REPORT NUMBER(S)
6a. NAME OF PERFORMING ORGANIZATION USAEWES Hydraulics Laboratory 6b. OFFICE SYMBOL (If applicable) CEWES-HE-E	7a. NAME OF MONITORING ORGANIZATION
6c. ADDRESS (City, State, and ZIP Code) 3909 Halls Ferry Road Vicksburg, MS 39180-6199	7b. ADDRESS (City, State, and ZIP Code)
8a. NAME OF FUNDING/SPONSORING ORGANIZATION USAED, New Orleans 8b. OFFICE SYMBOL (If applicable)	9. PROCUREMENT INSTRUMENT IDENTIFICATION NUMBER
8c. ADDRESS (City, State, and ZIP Code) PO Box 60267 New Orleans, LA 70160-0267	10. SOURCE OF FUNDING NUMBERS PROGRAM ELEMENT NO. / PROJECT NO. / TASK NO. / WORK UNIT ACCESSION NO.

11. TITLE (Include Security Classification)

An Analysis of Training Structure Designs in Southwest Pass, Mississippi River

12. PERSONAL AUTHOR(S)

Heltzel, S. B.; Martin, W. D.; Berger, R. C.; Richards, D. R.

13a. TYPE OF REPORT	13b. TIME COVERED	14. DATE OF REPORT (Year, Month, Day)	15. PAGE COUNT
Final report	FROM ____ TO ____	November 1989	53

16. SUPPLEMENTARY NOTATION

Available from National Technical Information Service, 5285 Port Royal Road, Springfield, VA 22161.

17. COSATI CODES			18. SUBJECT TERMS (Continue on reverse if necessary and identify by block number)
FIELD	GROUP	SUB-GROUP	Currents; Dike; Navigation channel; Numerical model; Sedimentation

19. ABSTRACT (Continue on reverse if necessary and identify by block number)

The Southwest Pass of the Mississippi River is the main navigation outlet to the Gulf of Mexico. As a part of planned efforts to stabilize the banks of the Southwest Pass and reduce maintenance dredging, improvements on the lower part of the river near the entrance were being reviewed due to the significant costs of this portion, in particular, the concrete pile inner bulkhead in the jetty reach.

This report details an investigation which had as its primary objective to produce an alternative design which is lower in construction costs and provides comparable reduction of channel sedimentation relative to the inner bulkhead plan. This objective was undertaken by consideration of plans which modify the existing dike fields along the Southwest Pass channel.

(Continued)

20. DISTRIBUTION/AVAILABILITY OF ABSTRACT ☒ UNCLASSIFIED/UNLIMITED ☐ SAME AS RPT ☐ DTIC USERS	21. ABSTRACT SECURITY CLASSIFICATION Unclassified
22a. NAME OF RESPONSIBLE INDIVIDUAL	22b. TELEPHONE (Include Area Code) / 22c. OFFICE SYMBOL

DD Form 1473, JUN 86 Previous editions are obsolete.

SECURITY CLASSIFICATION OF THIS PAGE

Unclassified

Unclassified

SECURITY CLASSIFICATION OF THIS PAGE

19. ABSTRACT (Continued).

Seven plans (Plans A-G) and existing conditions were evaluated using the TABS-2 finite element numerical model RMA-2V to provide the flow fields and the Memphis District method and Colby's method for sediment transport capacities. The plan dike fields were developed as a logical progression by consideration of the uniformity of the longitudinal channel velocity and sediment transport capacity.

Results indicate that the important element is the extension of the dike fields back to the jetty to prevent flow out of the channel and behind the dikes. Plan E, which involves the extension of only six existing dikes, provides nearly the same velocity profile and transport capacity as the inner bulkhead design (Plan G) at a fraction of the construction costs. Thus this plan is the recommended design.

Unclassified

SECURITY CLASSIFICATION OF THIS PAGE

PREFACE

In January 1988, the US Army Engineer District, New Orleans, requested that the US Army Engineer Waterways Experiment Station (WES) conduct an investigation to assess general changes in hydrodynamics and sedimentation associated with two plans to reduce shoaling in Mississippi River Southwest Pass, Louisiana.

The study was conducted by personnel of the Hydraulics Laboratory, WES, under the general direction of Messrs. F. A. Herrmann, Jr., Chief of the Hydraulics Laboratory; R. A. Sager, Assistant Chief of the Hydraulics Laboratory; W. H. McAnally, Jr., Chief of the Estuaries Division; and W. D. Martin, Chief of the Estuarine Engineering Branch. The project was conducted by Messrs. S. B. Heltzel, D. R. Richards, and W. D. Martin, Estuarine Engineering Branch, and R. C. Berger of the Estuaries Division. This report was prepared by Messrs. Heltzel, Martin, Berger, and Richards and was edited by Mrs. Marsha C. Gay of the Information Technology Laboratory, WES. Mr. Cecil Soileau of the US Army Engineer District, New Orleans, provided valuable technical consultation.

Acting Commander and Director of WES during preparation of this report was LTC Jack R. Stephens, EN. Technical Director was Dr. Robert W. Whalin.

CONTENTS

CONVERSION FACTORS, NON-SI TO SI (METRIC)
UNITS OF MEASUREMENT

Non-SI units of measurement used in this report can be converted to SI (metric) units as follows:

Multiply	By	To Obtain
cubic feet	0.02831685	cubic metres
feet	0.3048	metres
square fect	0.09290304	square metres

AN ANALYSIS OF TRAINING STRUCTURE DESIGNS IN SOUTHWEST PASS, MISSISSIPPI RIVER

PART I: INTRODUCTION

Southwest Pass

1. The Southwest Pass of the Mississippi River is the main navigation outlet to the Gulf of Mexico, as shown in Figure 1. Historically, it has undergone many physical changes by man to improve its ability to provide safe and economical navigation to the interior United States. Typically, the changes were efforts to reduce the costs of maintaining the deepened navigation channels and to protect the Pass against attack by waves and subsidence.

2. Recently, the US Army Engineer District, New Orleans, developed a plan that would assist in stabilizing the banks of Southwest Pass from erosion while providing a hydraulic environment in the navigation channel that would require less maintenance dredging. The planned improvements to Southwest Pass are described in detail in the General Design Memorandum (GDM) (US Army Engineer District, New Orleans, 1984).

3. Much of the plan had been built at the time of this study, but the improvements on the lowest part of the river near the entrance were being reviewed due to the significant costs of this portion. In particular, the concrete pile inner bulkhead in the jetty reach warranted a review of design alternatives.

Objectives

4. The objectives of this study were to determine if additional training dikes in the Southwest Pass jetty reach would provide training of the flows comparable to a complete closure between the inner bulkheads and jetties and thus provide equivalent maintenance dredging savings for significantly lower construction costs.

Study Design and Approach

5. A plan was developed that used numerical models to evaluate less

expensive alternatives. A total of eight geometries were tested. These are summarized in Table 1 and shown in Figures 2-9.

6. Because information from the New Orleans District indicated that the most important shoaling events occurred at flows above 900,000 cfs* at Venice, LA., it was agreed that only this flow would be tested for the purposes of comparing the base and seven plans. This flow effectively moves the salt wedge to the tip of the jetties so that the assumptions of a vertically averaged, homogeneous flow model are reasonable in the study area. Additionally, at these flows, sediment transport in the jetty reach is not strongly affected by tides, so only steady-state conditions were considered.

7. The most recent hydrographic survey sheets (dated 11 March 1988) were used to determine the existing depths in the area. Water depths outside the navigation channel were provided by surveys conducted within the jetties. Drawings that depicted the terminus of the constructed portion of the GDM features were used to further define the geometry of the study area.

8. Finite element meshes were constructed for each of the eight desired geometries. The same mesh was used for each condition with dikes being modeled by changing the particular dike element from a fluid element to a solid one. Since identical depths and boundary conditions were used for each simulation, the differences in the results came from the dike positioning alone. The TABS-2 numerical modeling system was then used for both hydrodynamic and sediment transport simulations. This system has been used on several previous studies in this area and has proven a reliable tool for analysis. The scope of the subject study did not permit verification of the TABS model. However, this was unnecessary because the results were used to make qualitative comparisons between the eight conditions and not quantitative comparisons. Anomalous results from the sediment numerical model resulted in its replacement with an analytical method.

9. Sediment transport capacities were calculated using the Memphis District equation, a modified form of Ilo's equation (Ilo 1975), and Colby's method (Colby 1964). Since the study purpose was not to quantify the differences in the conditions analyzed, but rather to evaluate them qualitatively, this analytical approach was appropriate. Inclusion of this analytical method

* A table of factors for converting non-SI units of measurement to SI (metric) units is found on page 3.

provided an additional source of information from which to determine the relative performance of the eight conditions evaluated.

PART II: NUMERICAL MODELING

TABS-2 Modeling System

10. TABS-2 is a family of computer programs used in two-dimensional (2-D) modeling of hydrodynamics, sedimentation, and constituent transport in rivers, reservoirs, bays, and estuaries. The system was developed by the Hydraulics Laboratory, US Army Engineer Waterways Experiment Station, using the finite-element, hydrodynamic model, RMA-2V, and sediment transport model, STUDH. Significant enhancements to the codes, as well as development of pre- and postprocessing utilities, have allowed for applications to a wide class of computational hydraulics problems. A more detailed description of both models appears in Appendix A.

Numerical Hydrodynamic Model

Mesh design

11. A 2-D mesh was designed to represent the Southwest Pass from below mile 16 at dike 16.29L to the entrance. Hydrographic surveys of Southwest Pass, Louisiana, taken by the New Orleans District, sheets 9 and 10 dated 11 March 1988, were used to design the numerical model mesh. The mesh shown in Figure 10 contained 2,175 elements and 6,796 nodes and included elements to define the existing and proposed lateral dikes. Depths at each node were assigned using recent surveys from the New Orleans District.

12. The upper portions of Figures 2-9 show the dike configuration for each case, and the lower portions show the resulting velocity fields. The base plan was derived from the hydrographic surveys of Southwest Pass, Louisiana, which show the locations and lengths of existing dikes. The locations of the east and west jetties, also defined by these surveys, determined the lateral extent of the model (Figure 2). Plan A (Figure 3) consisted of adding supplemental dikes between existing dikes with no other conditions altered. Most of these dikes were detached from the jetties. Plan B (Figure 4) connected five selected dikes from Plan A on the right bank. Plan C (Figure 5) connected 10 selected dikes from Plan A to the jetties. Five were on the right bank and five on the left bank. Plan D (Figure 6) connected four of the dikes from Plan A to the jetties, three on the left bank, and one on the right

bank. Plan E (Figure 7) connected six of the base condition dikes to the jetties, four on the left bank and two on the right bank. Plan F (Figure 8), the minimum structural alternative, connected two of the base dikes on the right bank and one of the additional lateral dikes from Plan A to the right jetty. Plan G (Figure 9) included the existing dike locations and lengths from the inner east-west bulkhead toward the channel. Everything behind the bulkhead is considered solid and flow does not pass through it.

Testing conditions

13. The model was run with a turbulent exchange coefficient of 20 ft^2/sec and Manning's n friction values varying between 0.020 and 0.030. The friction values were based on depth. A 900,000-cfs flow at Venice, LA, was duplicated for this study. Earlier studies indicated that with bank protection works described as Supplement 2 for the 40-ft-deep project in place, the Southwest Pass would convey 19 percent of the total 900,000-cfs discharge at Venice through the jetty reach (Richards and Trawle 1988). Based on this, velocity values were assigned to the upstream boundary and a mean water-surface elevation was assigned to the downstream boundary nodes and the model run in a steady-state mode.

Numerical Sediment Transport Model

14. The computational mesh for the sediment transport computations was identical to that of the hydrodynamic model. The base condition and Plans A and G were evaluated with the STUDH model. The length of the sedimentation model time-step selected was 1,800 sec (0.5 hr). Other model parameters were as follows:

Crank-Nicholson implicitness factor	0.66
Manning's n roughness	0.02
Effective particle diameter for transport	0.15 mm
Effective settling velocity	0.0075 m/sec
Upstream boundary concentration	0.10 kg/m^3
Dispersion coefficient	0.20 m^2/sec

15. The model was run in the following sequence:

a. Run 1 (10 time-steps): cold-start (set to zero) bed change and concentration.

b. Run 2 (10 time-steps): cold-start bed change and hot-start concentration from run 1.

c. Run 3 (1 time-step): cold-start bed change and hot-start concentration.

Sensitivity Testing

16. Sensitivity tests were conducted with the sediment transport model to determine those model parameters that produced the smallest reasonable bed change during a time-step. A smaller version of the mesh from river mile 19.05 to the entrance was used in this evaluation. Initially an effective particle diameter for transport of 0.15 mm and an upstream boundary concentration of 0.10 kg/m^3 were assigned to determine the lowest value for the dispersion coefficient that could be used to produce meaningful results with the model. The model was run with dispersion coefficients of 1.0, 0.5, and 0.1 m^2/sec. The value of 0.1 m^2/sec did not produce concentration oscillations at this point; but in some of the later tests, the flow fields were more difficult and oscillations occurred for values below 0.2 m^2/sec. This value, 0.2, was used for all testing. Finally, the incoming sediment concentration was varied using values of 0.5 kg/m^3 and 0.9 kg/m^3 and the results showed no improvement. The results also showed that the model required at least the upper one-third of the mesh to initially reach some equilibrium and produce reasonable results. Therefore the model mesh was extended upstream to move this transition region away from the study area. The test also showed that the downstream boundary was appropriate for this study.

Analytical Sediment Transport Analysis

17. The Memphis District and Colby sediment transport relationships were selected to provide additional insight into the relative merits of the conditions tested. The Memphis District equation is a stream power type equation that also considers the slope of the energy grade line. It was developed by G. W. Forney, Jr., and W. D. Martin for application in the US Army Engineer District, Memphis. It is a modified version of Ilo's equation (Ilo 1975). The slope in the equation is taken to be equal to the water-surface slope for large rivers such as the Mississippi. The equation is presented as follows:

$$Q_s = \frac{(0.25 * Q_w * V * V * S)}{d_{65}} \qquad (1)$$

where

Q_s = sediment transport, tons per day

Q_w = water discharge, cfs

V = average cross-sectional velocity, fps

S = slope, ft per ft

d_{65} = grain size, ft, for which the bed material is 65 percent finer by weight

This method was used to evaluate the base condition and Plans A and G.

18. Colby's relationship applies to sand-size material with a d_{50} between 0.1 and 1.0 mm. The relationship consists of four graphs and gives the uncorrected sediment discharge as a function of average cross-sectional velocity, water depth, and the median grain size of the material found in the riverbed. Additional graphs correct for temperature, fine sediment concentration, and median size of bed sediment (Colby 1964). These calculations were made using the CORPS system for engineering design (Jones 1977). This method was used to evaluate the base condition and Plans A and G. It was then compared with the Memphis District results. Based on this comparison of the two analytic methods, Colby's relationship was selected as the basis for qualitative comparison of the performance of all eight geometries tested.

19. The input variables for these equations were obtained from the TABS-2 hydrodynamic results for the various conditions evaluated. These are summarized in Table 2.

PART III: RESULTS AND CONCLUSIONS

Hydrodynamics

20. The hydrodynamic results for the base and seven plans are discussed in this section. Velocity magnitudes and surface elevations along the channel center line were compared, and the 2-D vector plots of velocities were developed.

Velocity magnitudes

21. Velocity magnitudes were compared along the channel center line at locations adjacent to existing dikes and proposed lateral dikes and midway between them. A channel cross-section weighted average velocity for each location was calculated by giving the velocities at locations adjacent to the dikes a weight of 1/6 and the velocity of the center line of the channel a weight of 2/3. This weighting reasonably reflects the appropriate average flow velocities profile in a simple manner. Table 3 is a tabulation of these weighted average velocity magnitudes. Figure 11 is a plot of these values along the channel center line. In general, velocities were modified least by Plan A, although some increase across the channel was noted. Plan G caused the greatest impact on velocities. This was a result of a complete blockage of flow around the landward ends of the dikes near the model boundary. Model results near a flow boundary are generally less reliable; thus, the proximity of the lower boundary may indicate that the predicted drop in velocity there is a numerical artifact rather than an actual difference. Plan E provided results virtually identical to Plan G.

Velocity results

22. The velocity vectors for the base condition and Plans A through G are shown in the lower portion of Figures 2 through 9. It can be seen that in all plans other than C, E, and G, there is significant flow behind the dikes (between the dikes and jetties). This criterion was used during testing to determine which dikes should be extended. Thus by reducing the flow bypassing the dike fields, the channel velocities were increased.

23. The various plans resulted in local variations in the weighted velocities as measured at the cross sections shown in Table 3. These results are more readily interpreted from Figure 11, which shows them graphically. It can be seen that Plan G, the inner bulkhead plan, provides the highest

velocities in the study reach. The various other plans generally fall below the Plan G plot, indicating lower velocities. Plan C, the alternative with the maximum number of dikes, resulted in velocities very near or slightly higher than Plan G. Plan E, which connected four existing base condition dikes on the left bank and two on the right bank to the jetties, resulted in velocities only slightly lower than Plans G and C. The remainder of the plans were all inferior to Plans G, C, and E.

Water-surface elevations

24. Water-surface elevations were compared at the same locations as the velocity magnitudes. The greatest variation observed between the plans was less than 0.05 ft. Therefore, the water-surface elevations were considered unchanged by the various plans.

Sedimentation

Numerical results

25. As previously mentioned in paragraph 16, the numerical model was tested for sensitivity to changes in the variables to ensure that the results were reasonable. This testing was necessitated by the fact that the model was not verified. When this portion of the study was completed, the model appeared to be producing reasonable shoaling patterns that would be expected in the study area.

26. However, when Plans A and G were evaluated in the numerical model, the results were inconsistent with the expected shoaling trend. The plans appeared to increase channel shoaling in the study area. This was contrary to what would be expected with an increase in velocities and more uniform channel streamlines as determined by the hydrodynamic results. The scope of the study did not allow resolution of this anomaly (though it is suspected to be due to the assumption of uniform velocity and concentration vertically in a 2-D model), and no further plans were evaluated with the sediment model.

Analytical results

27. The analytical results were based upon analysis of the sediment transport potential for the three conditions and evaluation of the variation in velocities and water-surface slopes. All evaluations were made by comparing the plan results with the base results. The Memphis District formula proved to be a poor predictor due to sensitivity of this equation to slight

changes in slope; therefore, it was not used in the complete analysis. The Colby formula seemed to provide the most reasonable and consistent results. The Colby variables used in the analysis are as follows:

Water discharge	162,000 cfs
D_{65} grain size	0.15 mm
Water depth	40 ft
Channel water width	900 ft
Fine material concentration	150 parts per million
Water velocity	As shown in Table 2

The Colby results are discussed below.

Sediment transport results

28. While the sediment transport varied from reach to reach, the total sediment transport was very similar for all of the plans. The incremental and cumulative sediment transport capacity by reach for each plan is shown in Table 3. Plan C resulted in the greatest cumulative sediment transport capacities in the study reach. Plans E and G provided similar cumulative sediment transport capacities, both of which were slightly less than the Plan C results. The transport capacities for the remaining plans were all lower than the results for Plans C, E, and G. The results for each plan are summarized in the following tabulation showing the increase in cumulative sediment transport as a percent when compared to the base condition. Figure 12 shows the results for each plan graphically.

Plan	Change in Cumulative Sediment Transport Capacity, percent
Base	0.00
A	+1.00
B	+3.00
C	+7.00
D	+2.00
E	+4.00
F	+2.00
G	+4.00

PART IV: CONCLUSIONS

29. The following conclusions are based on the qualitative comparison of results from the numerical and analytical analyses.

a. Plans C, E, and G provided the most uniform streamlines within the study reach.

b. The improved streamlines for Plans C and E should reduce erosion of the submerged berms on either side of the navigation channel. Plan G, with the inner bulkhead, completely shelters the berms.

c. The velocities were highest and very similar for Plans C, E, and G.

d. Plan C resulted in the greatest increase in total sediment transport capacity within the study reach -- 7 percent over the base condition. Plans E and G were the next most efficient sediment transport schemes with increases of 4 percent over the base condition.

e. While a quantitative economic evaluation of the plans is beyond the scope of this study, it would appear that Plan E (extension of six existing dikes), which requires considerably fewer structural additions to the existing Southwest Pass features than either Plan C or G, provides the best and most economical results. Plan C calls for the construction of 22 additional dikes and the extension of 10 additional dikes. Plan G calls for an inner bulkhead of continuous concrete piles to be constructed within the entire length of the study area.

f. Based on maximizing increases in velocity and sediment transport and minimizing structural additions, Plan E is recommended as the best overall plan evaluated.

REFERENCES

Colby, B. R. 1964. "Practical Computation of Bed Material Discharge," Journal, Hydraulics Division, American Society of Civil Engineers, Vol 90, No. HY2, pp 217-246.

Ilo, H. 1975. "Sediment Transport in Streams," Journal Hydraulics Division, American Society of Civil Engineers, Vol 101, No. HY12, pp 1559-1565.

Jones, H. W. 1977 (Jun). "Manual for a Conversationally Oriented Real-Time Program Generating System (CORPS)," US Army Engineer Waterways Experiment Station, Vicksburg, MS.

Richards, D. R., and Trawle, M. J. 1988 (Sep). "A Numerical Model Analysis of Mississippi River Passes Navigation Channel Improvements; 45-Foot Channel Tests and Flow Diversion Schemes," Miscellaneous Paper HL-87-2, Report 2, US Army Engineer Waterways Experiment Station, Vicksburg, MS.

US Army Engineer District, New Orleans. 1984 (Apr). "General Design Memorandum, Mississippi River, Baton Rouge to the Gulf of Mexico, Louisiana, Southwest Pass and Bar Channel," New Orleans, LA.

Table 1

Alternatives Tested

Nomenclature	Features	Comments
Base	Existing dikes	With Supplement 2 training works in place
Plan A	Double the existing dikes	Not all connected to jetties
Plan B	5 dikes connected to jetty	All on right bank
Plan C	5 left bank, 5 right bank dikes connected to jetties	Otherwise, same as Plan A
Plan D	3 left bank, 1 right bank dikes connected to jetties	Otherwise, same as base
Plan E	4 left bank, 2 right bank dikes connected to jetties	Otherwise, same as base
Plan F	3 right bank dikes connected to jetty	2 base dikes, one additional lateral dike
Plan G	Inner continuous bulkhead	General Design Memorandum Plan

Table 2

River Velocity, fps

Mile	Left	Center	Right	Arithmetic Average	Weighted Average
			Base		
17.80	3.0	3.2	3.0	3.1	3.2
18.02	3.2	3.6	3.3	3.4	3.5
18.40	2.8	3.4	3.4	3.2	3.3
18.62	2.2	3.6	3.6	3.1	3.3
18.83	1.5	3.6	3.7	2.9	3.3
19.05	1.9	3.5	3.6	3.0	3.3
19.27	2.0	3.6	3.6	3.1	3.3
19.59	2.1	3.7	3.7	3.1	3.4
19.80	2.3	3.9	3.7	3.3	3.6
20.00	2.6	3.9	3.6	3.4	3.6
20.14	2.4	3.9	3.7	3.3	3.6
			Plan A		
17.80	3.1	3.4	3.1	3.2	3.3
18.02	3.1	3.5	3.2	3.3	3.4
18.40	2.7	3.5	3.5	3.2	3.4
18.62	1.9	3.6	3.7	3.1	3.4
18.83	1.5	3.6	3.7	2.9	3.3
19.05	1.7	3.6	3.6	2.9	3.3
19.27	1.9	3.6	3.7	3.1	3.3
19.59	2.0	3.7	3.7	3.1	3.4
19.80	2.2	3.9	3.7	3.3	3.6
20.00	2.5	4.0	3.6	3.4	3.7
20.14	2.3	4.0	3.7	3.3	3.6
			Plan B		
17.80	3.1	3.4	3.1	3.2	3.3
18.02	3.1	3.5	3.2	3.3	3.4
18.40	2.7	3.5	3.5	3.2	3.4
18.62	1.9	3.7	3.7	3.1	3.4
18.83	1.5	3.7	3.8	3.0	3.4
19.05	1.7	3.7	3.7	3.0	3.3
19.27	1.9	3.7	3.7	3.1	3.4
19.59	2.0	3.7	3.7	3.1	3.4
19.80	2.2	3.9	3.7	3.3	3.6
20.00	2.6	3.9	3.6	3.4	3.7
20.14	2.3	4.0	3.7	3.3	3.6

(Continued)

Table 2 (Continued)

Mile	Left	Center	Right	Arithmetic Average	Weighted Average
			Plan C		
17.80	3.1	3.4	3.1	3.2	3.3
18.02	3.2	3.5	3.3	3.3	3.4
18.40	2.7	3.6	3.6	3.3	3.5
18.62	2.0	3.8	3.8	3.2	3.5
18.83	1.6	3.7	3.8	3.0	3.4
19.05	1.8	3.7	3.7	3.1	3.4
19.27	1.9	3.7	3.7	3.1	3.4
19.59	2.0	3.7	3.7	3.1	3.4
19.80	2.2	3.9	3.7	3.3	3.6
20.00	2.6	4.0	3.6	3.4	3.7
20.14	2.3	4.0	3.7	3.3	3.6
			Plan D		
17.80	3.0	3.2	3.0	3.1	3.2
18.02	3.1	3.5	3.3	3.3	3.4
18.40	2.8	3.6	3.5	3.3	3.4
18.62	2.2	3.7	3.8	3.2	3.5
18.83	1.7	3.6	3.7	3.0	3.3
19.05	2.2	3.5	3.5	3.1	3.3
19.27	2.0	3.6	3.6	3.1	3.3
19.59	2.1	3.7	3.6	3.1	3.4
19.80	2.3	3.9	3.7	3.3	3.6
20.00	2.6	3.9	3.6	3.4	3.6
20.14	2.6	3.9	3.7	3.3	3.6
			Plan E		
17.80	3.0	3.2	3.0	3.1	3.2
18.02	3.1	3.5	3.3	3.3	3.4
18.40	2.8	3.6	3.5	3.3	3.4
18.62	2.2	3.7	3.8	3.2	3.5
18.83	1.7	3.6	3.7	3.0	3.3
19.05	2.0	3.6	3.6	3.1	3.4
19.27	2.0	3.7	3.6	3.1	3.4
19.59	2.2	3.7	3.6	3.2	3.4
19.80	2.3	3.9	3.7	3.3	3.6
20.00	2.6	3.9	3.6	3.4	3.6
20.14	2.4	3.9	3.7	3.3	3.6

(Continued)

Table 2 (Concluded)

Mile	Left	Center	Right	Arithmetic Average	Weighted Average
			Plan F		
17.80	3.0	3.2	3.0	3.1	3.1
18.02	3.2	3.5	3.3	3.3	3.4
18.40	2.8	3.5	3.4	3.2	3.3
18.62	2.3	3.6	3.6	3.2	3.4
18.83	1.6	3.6	3.7	3.0	3.3
19.05	1.9	3.6	3.6	3.0	3.3
19.27	2.0	3.6	3.6	3.1	3.7
19.59	2.0	3.7	3.7	3.1	3.4
19.80	2.3	3.9	3.7	3.3	3.6
20.00	2.6	3.9	3.6	3.4	3.7
20.14	2.4	3.9	3.7	3.3	3.6
			Plan G		
17.80	3.0	3.2	3.0	3.1	3.2
18.02	3.1	3.5	3.3	3.3	3.4
18.40	2.8	3.5	3.5	3.3	3.4
18.62	2.2	3.7	3.7	3.2	3.6
18.83	1.8	3.7	3.7	3.1	3.4
19.05	2.2	3.7	3.6	3.2	3.4
19.27	2.0	3.7	3.7	3.1	3.4
19.59	2.2	3.7	3.6	3.2	3.4
19.80	2.7	3.9	3.6	3.4	3.6
20.00	2.9	3.8	3.3	3.3	3.5
20.14	2.9	3.8	3.6	3.4	3.6

Table 3

Weighted Velocities and Sediment Transport

River Mile	Average Weighted Velocity, fps	Incremental Sediment Transport, tons/day	Cumulative Sediment Transport, tons/days
		Base	
17.80	3.2	65,000	65,000
18.02	3.5	96,000	161,161
18.40	3.3	79,000	240,000
18.62	3.3	81,000	321,000
18.83	3.3	73,000	394,000
19.05	3.3	73,000	467,000
19.27	3.3	79,000	546,000
19.59	3.4	86,000	632,000
19.80	3.6	103,000	735,000
20.00	3.6	111,000	846,000
20.14	3.6	108,000	954,000
		Plan A	
17.80	3.3	75,000	75,000
18.02	3.6	82,000	157,000
18.40	3.4	84,000	241,000
18.62	3.3	81,000	322,000
18.83	3.3	75,000	397,000
19.05	3.3	73,000	470,000
19.27	3.3	81,000	551,000
19.59	3.4	87,000	638,000
19.80	3.6	104,000	742,000
20.00	3.6	114,000	856,000
20.14	3.6	112,000	968,000
		Plan B	
17.80	3.3	75,000	75,000
18.02	3.4	82,000	157,000
18.40	3.4	84,000	241,000

(Continued)

Table 3 (Continued)

River Mile	Average Weighted Velocity, fps	Incremental Sediment Transport, tons/day	Cumulative Sediment Transport, tons/days
		Plan B (Continued)	
18.62	3.4	86,000	327,000
18.83	3.4	82,000	409,000
19.05	3.3	79,000	488,000
19.27	3.4	84,000	572,000
19.59	3.4	86,000	658,000
19.80	3.6	103,000	761,000
20.00	3.7	113,000	874,000
20.14	3.6	111,000	985,000
		Plan C	
17.80	3.3	75,000	75,000
18.02	3.4	88,000	163,000
18.40	3.4	91,000	254,000
18.62	3.5	94,000	348,000
18.83	3.4	85,000	433,000
19.05	3.4	85,000	518,000
19.27	3.4	86,000	604,000
19.59	3.4	89,000	693,000
19.80	3.6	104,000	797,000
20.00	3.7	114,000	911,000
20.14	3.6	112,000	1,023,000
		Plan D	
17.80	3.2	65,000	65,000
18.02	3.4	88,000	153,000
18.40	3.4	88,000	241,000
18.62	3.8	94,000	335,000
18.83	3.3	80,000	415,000
19.05	3.3	76,000	491,000

(Continued)

Table 3 (Continued)

River Mile	Average Weighted Velocity, fps	Incremental Sediment Transport, tons/day	Cumulative Sediment Transport, tons/days
		Plan D (Continued)	
19.27	3.3	80,000	571,000
19.59	3.4	86,000	657,000
19.80	3.6	104,000	761,000
20.00	3.6	111,000	872,000
20.14	3.6	107,000	979,000
		Plan E	
17.80	3.2	65,000	65,000
18.02	3.4	88,000	153,000
18.40	3.4	88,000	241,000
18.62	3.5	94,000	335,000
18.83	3.3	80,000	415,000
19.05	3.4	85,000	500,000
19.27	3.4	84,000	584,000
19.59	3.4	88,000	672,000
19.80	3.6	104,000	776,000
20.00	3.6	111,000	887,000
20.14	3.6	109,000	996,000
		Plan F	
17.80	3.1	65,000	65,000
18.02	3.4	89,000	154,000
18.40	3.3	80,000	234,000
18.62	3.4	86,000	320,000
18.83	3.3	77,000	397,000
19.05	3.3	78,000	475,000
19.27	3.4	83,000	558,000
19.59	3.4	87,000	645,000
19.80	3.6	103,000	748,000

(Continued)

Table 3 (Concluded)

River Mile	Average Weighted Velocity, fps	Incremental Sediment Transport, tons/day	Cumulative Sediment Transport, tons/days
		Plan F (Continued)	
20.00	3.7	113,000	861,000
20.14	3.6	110,000	971,000
		Plan G	
17.80	3.2	65,000	65,000
18.02	3.4	87,000	152,000
18.40	3.4	87,000	239,000
18.62	3.5	92,000	331,000
18.83	3.4	82,000	413,000
19.05	3.4	87,000	500,000
19.27	3.4	84,000	584,000
19.59	3.4	90,000	674,000
19.80	3.6	109,000	783,000
20.00	3.5	101,000	884,000
20.14	3.6	112,000	996,000

(Sheet 4 of 4)

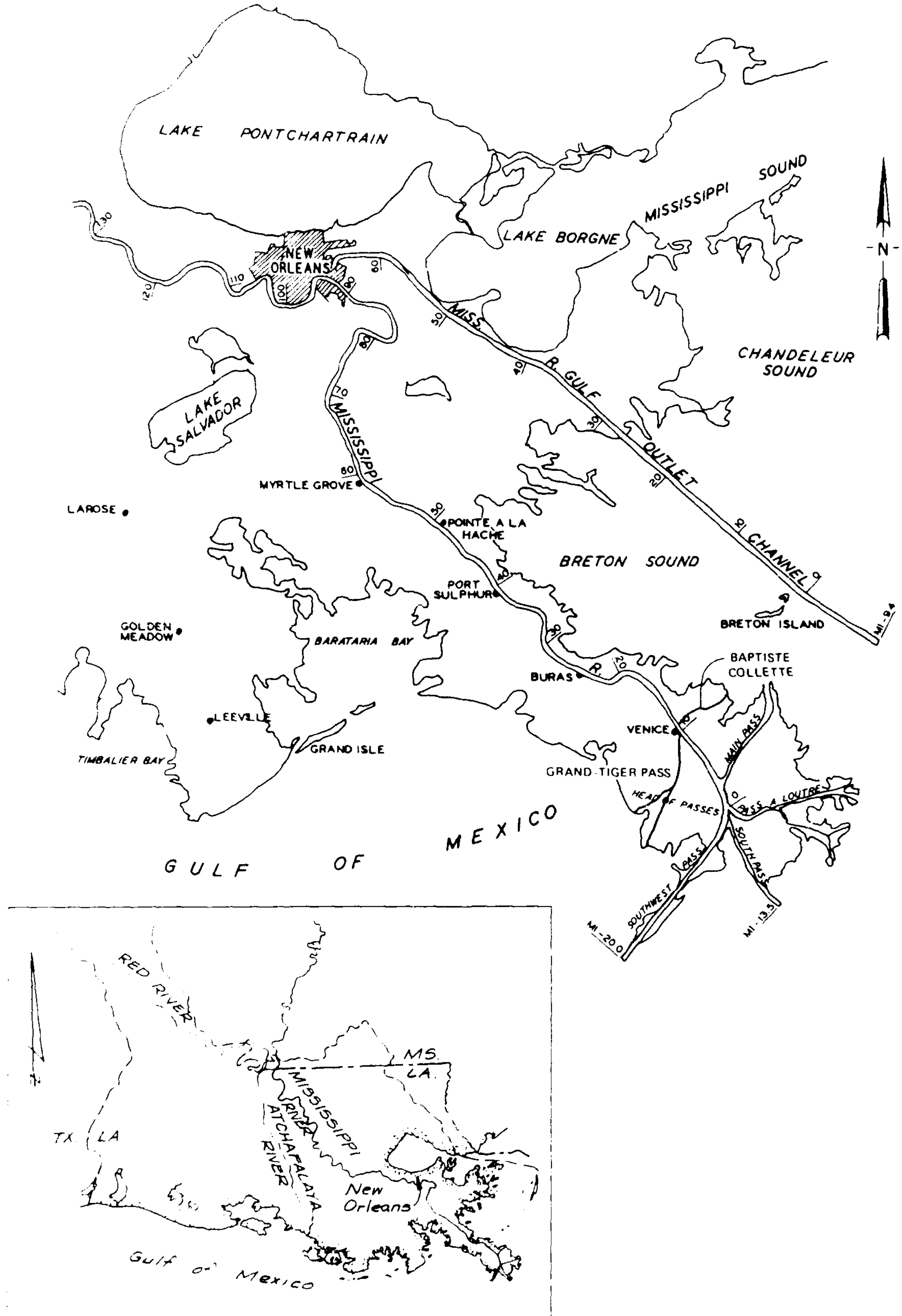

Figure 1. Location map

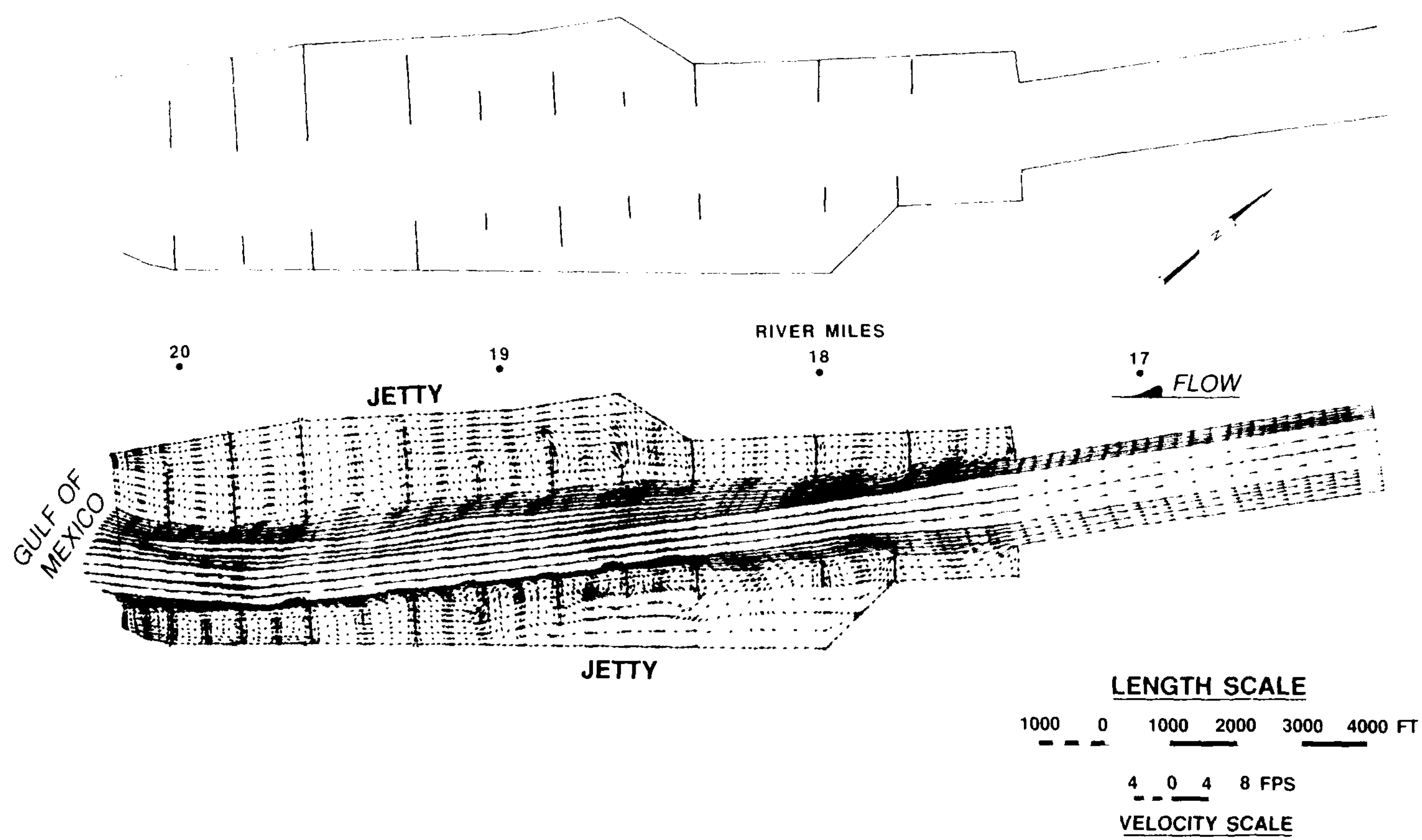

Figure 2. Base dike layout and velocity field

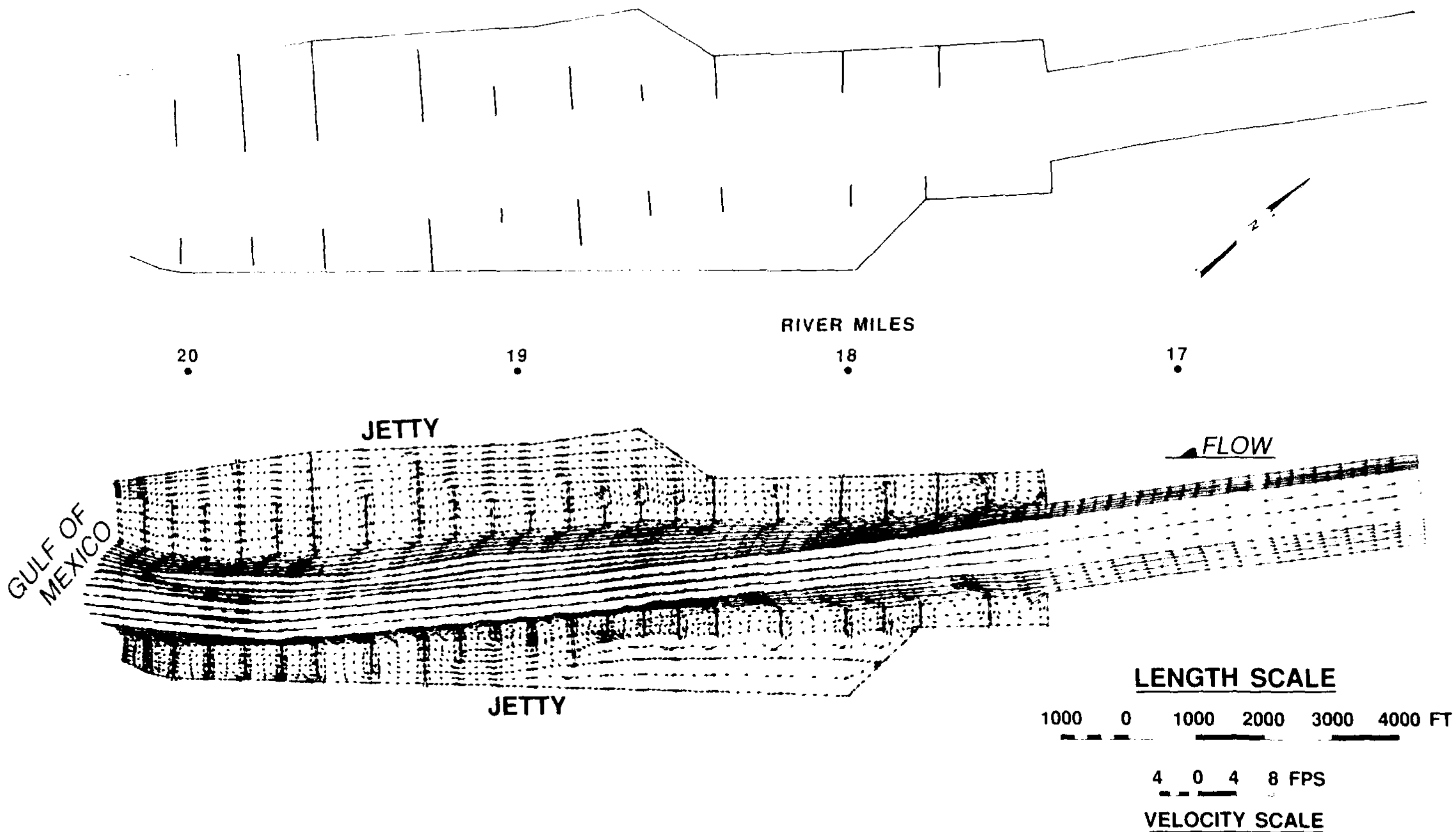

Figure 3. Plan A dike layout and velocity field

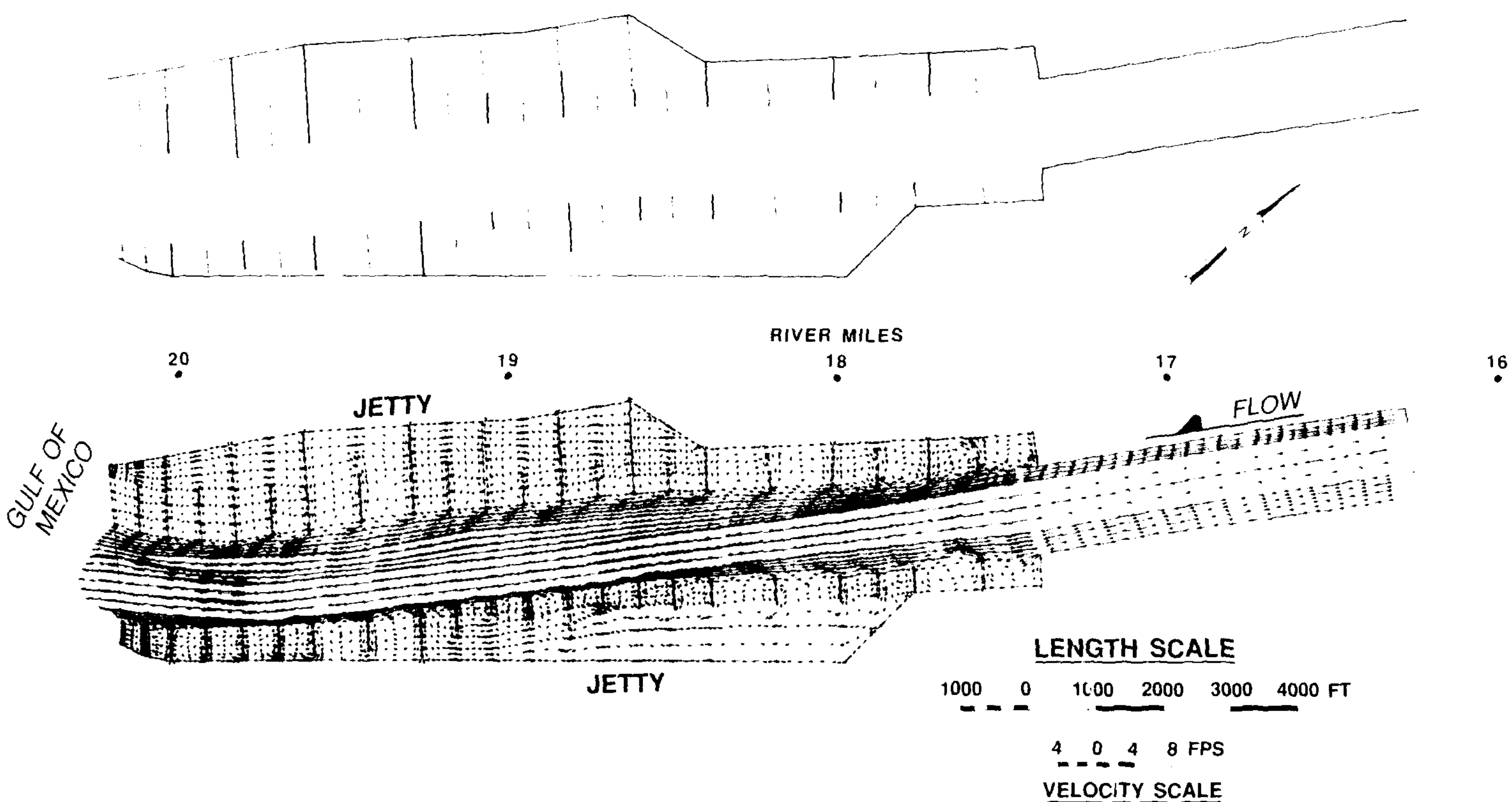

Figure 4. Plan B dike layout and velocity field

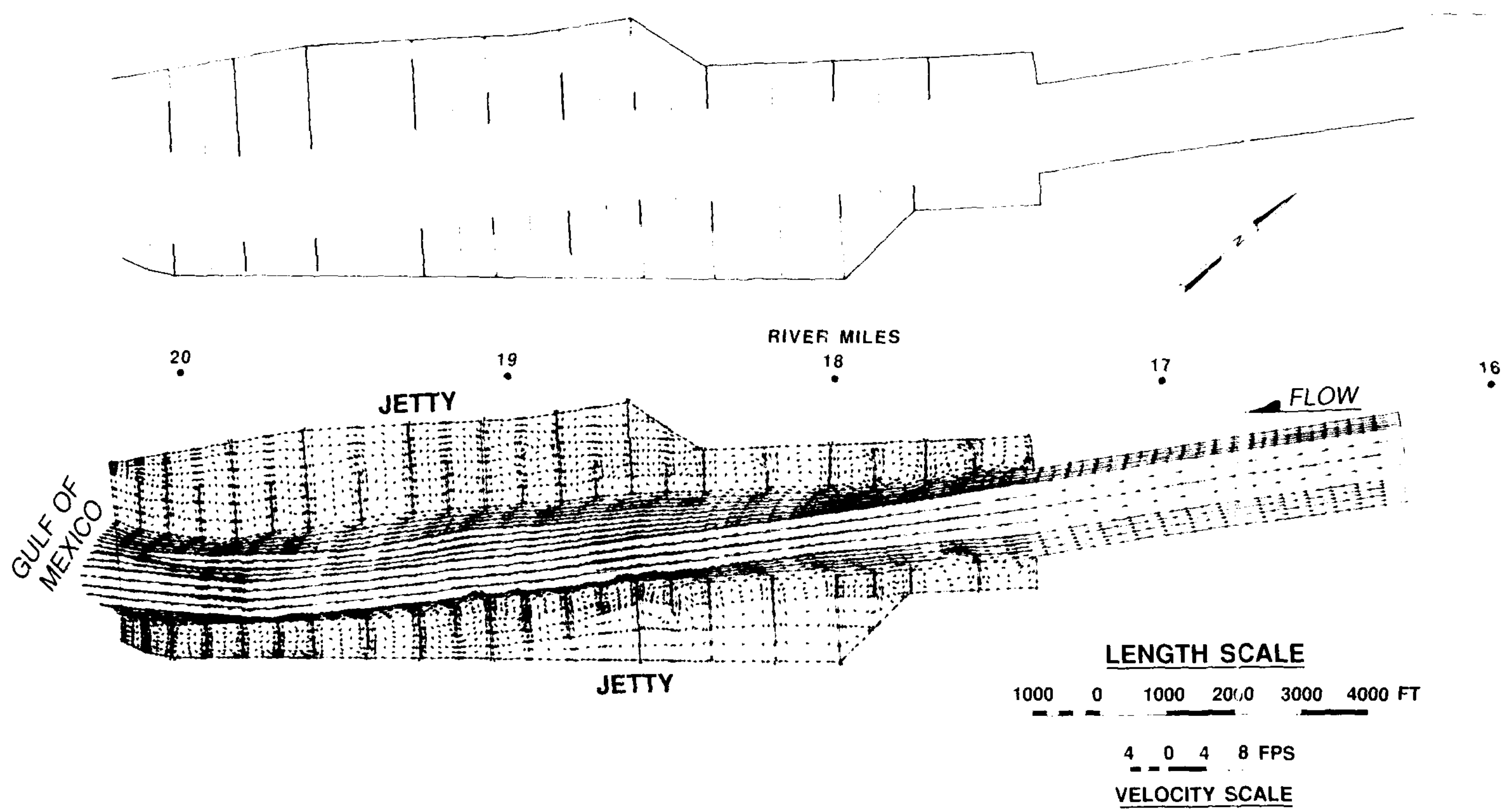

Figure 5. Plan C dike layout and velocity field

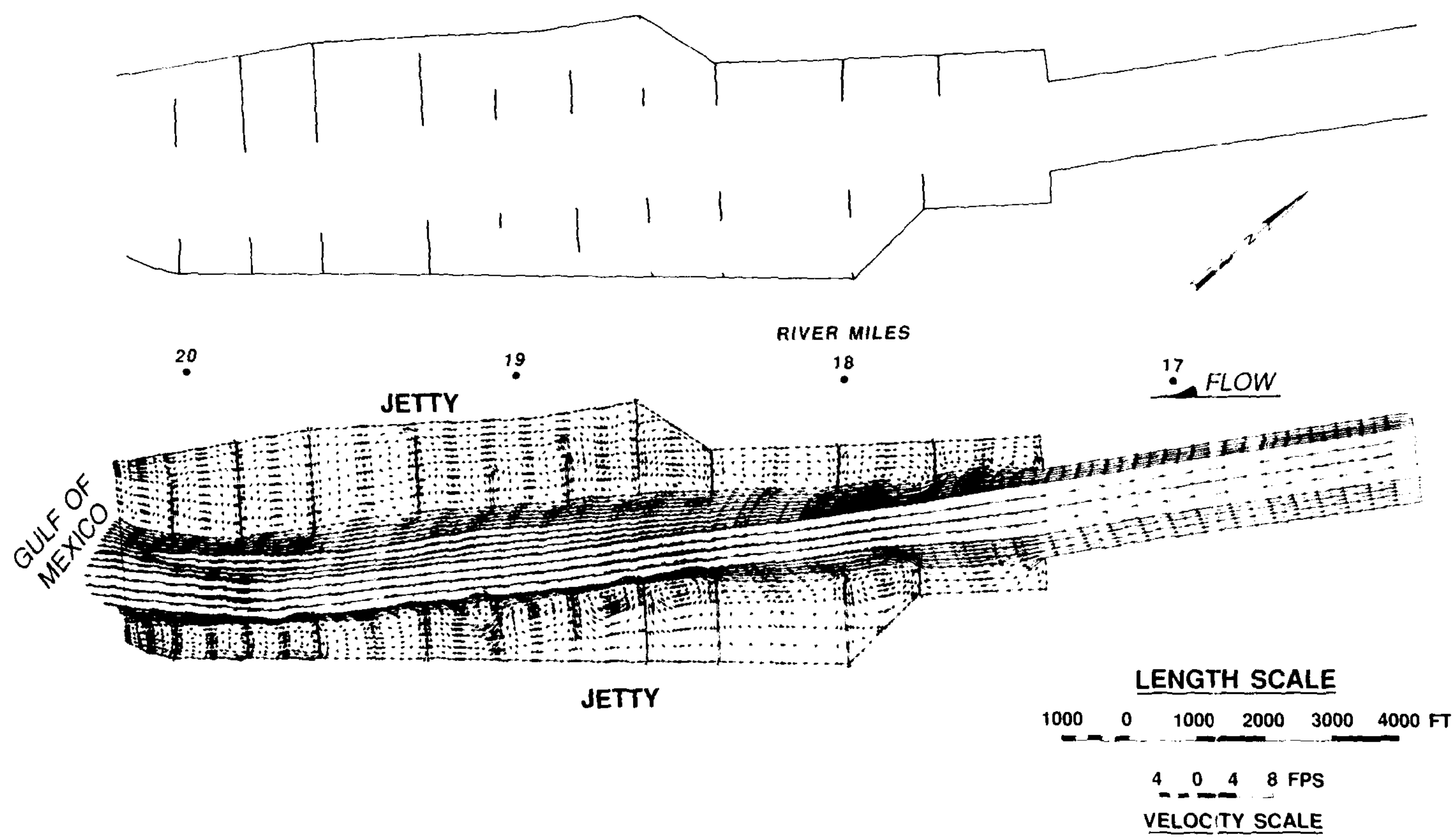

Figure 6. Plan D dike layout and velocity field

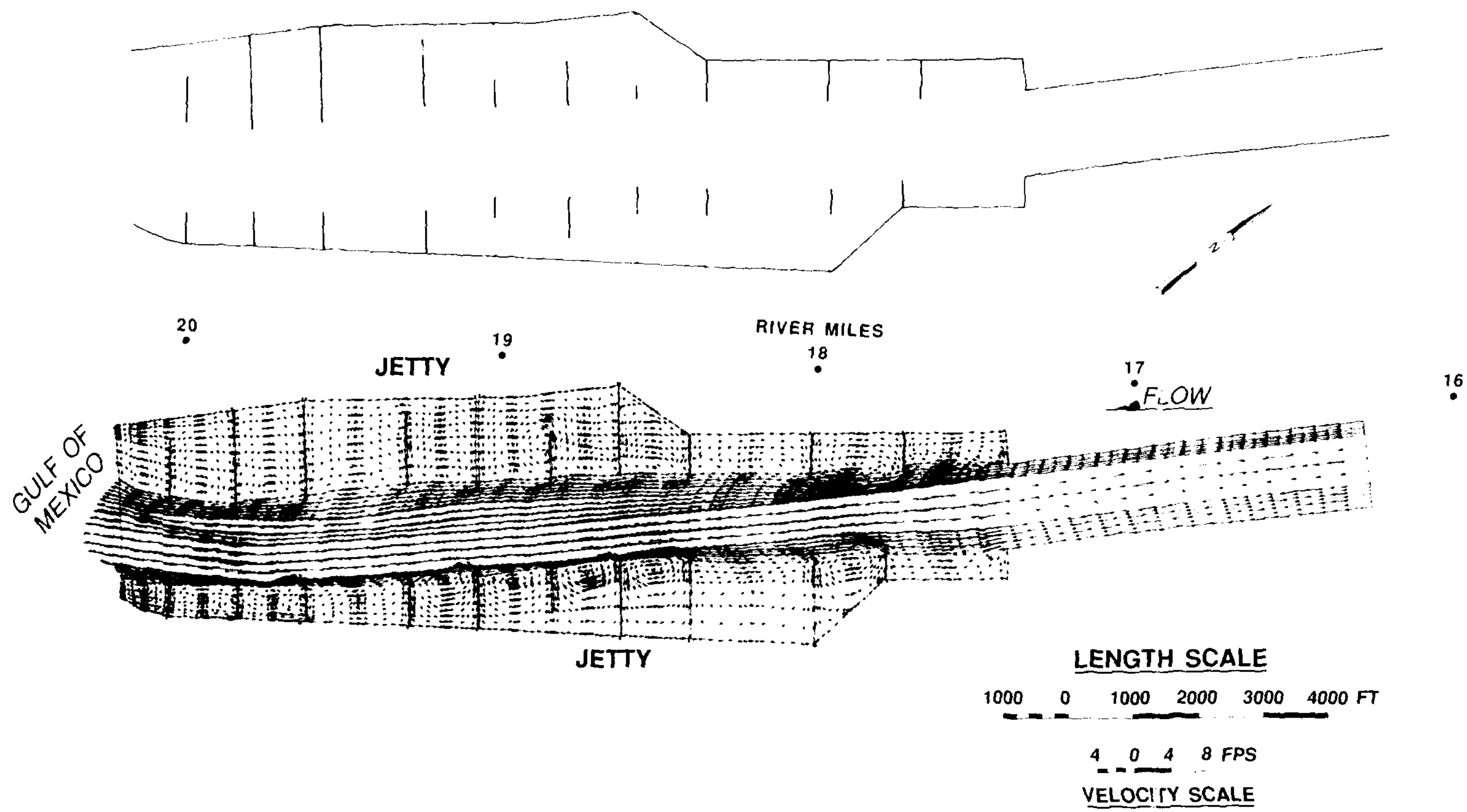

Figure 7. Plan E dike layout and velocity field

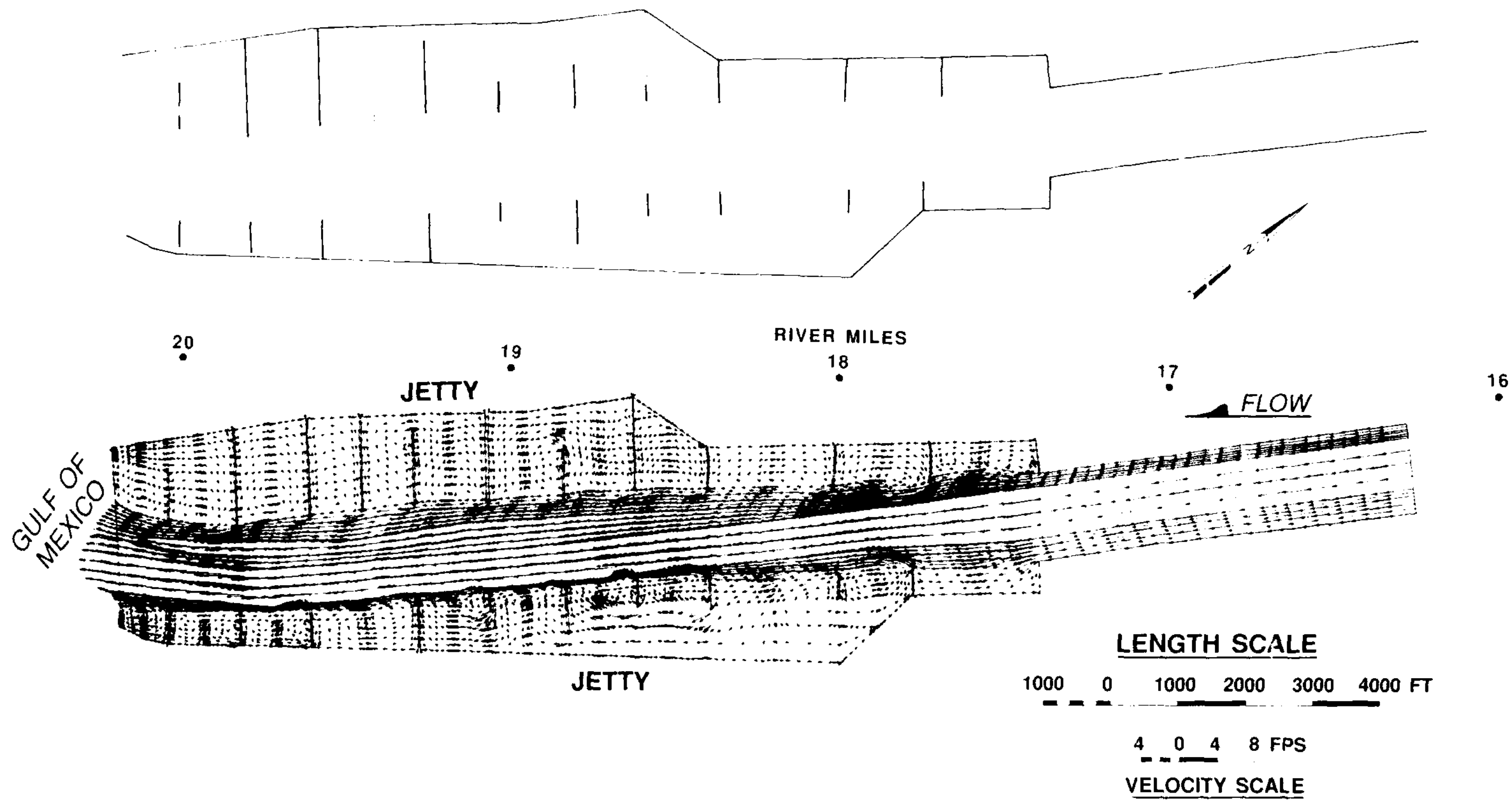

Figure 8. Plan F dike layout and velocity field

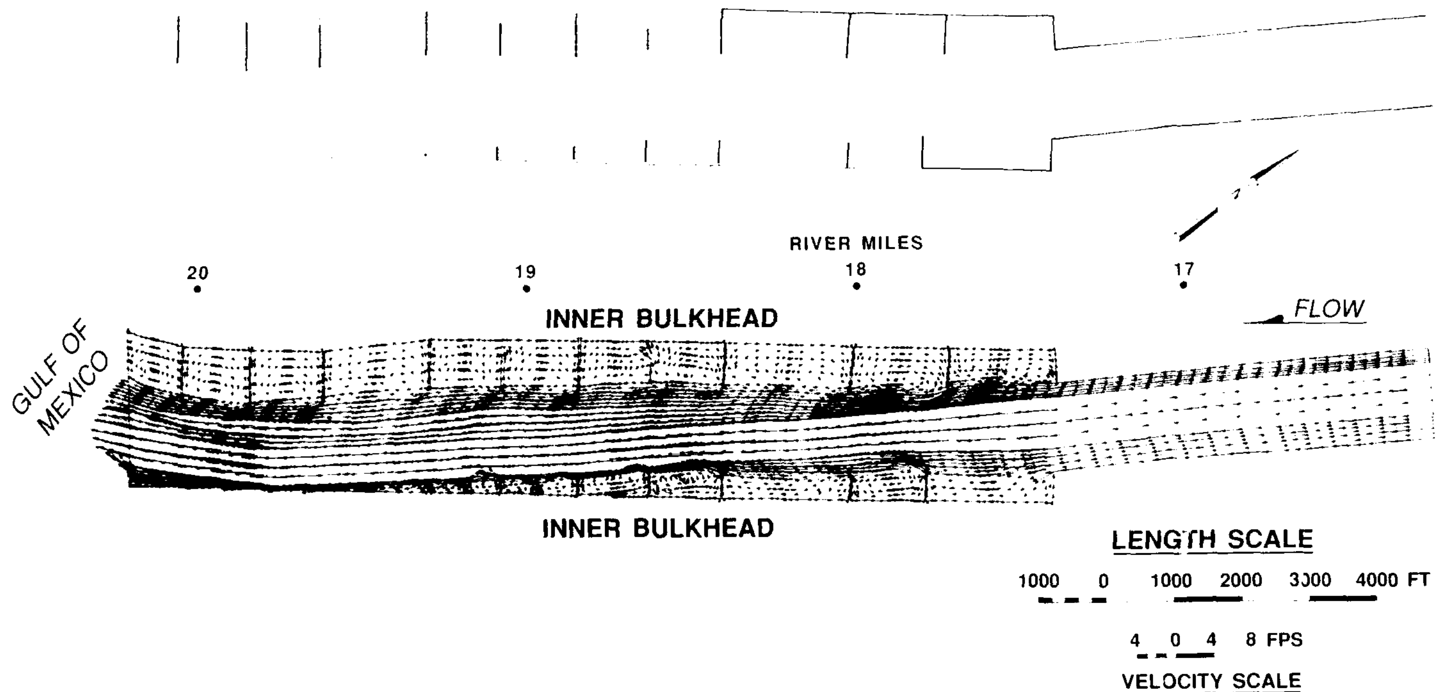

Figure 9. Plan G dike layout and velocity field

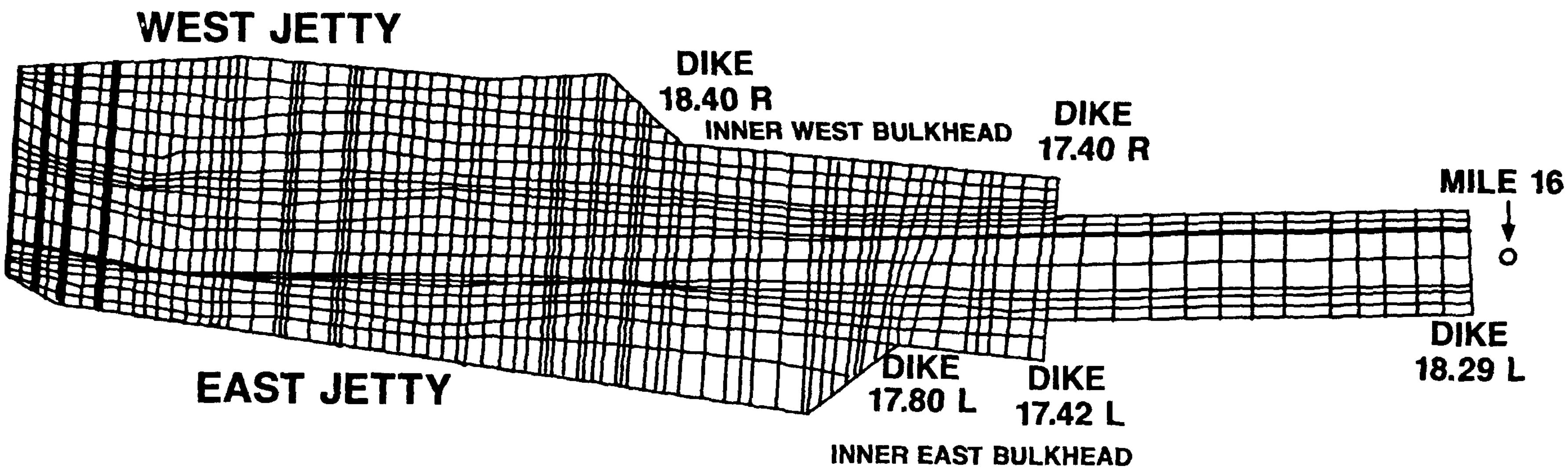

Figure 10. Lower Southwest Pass numerical model mesh

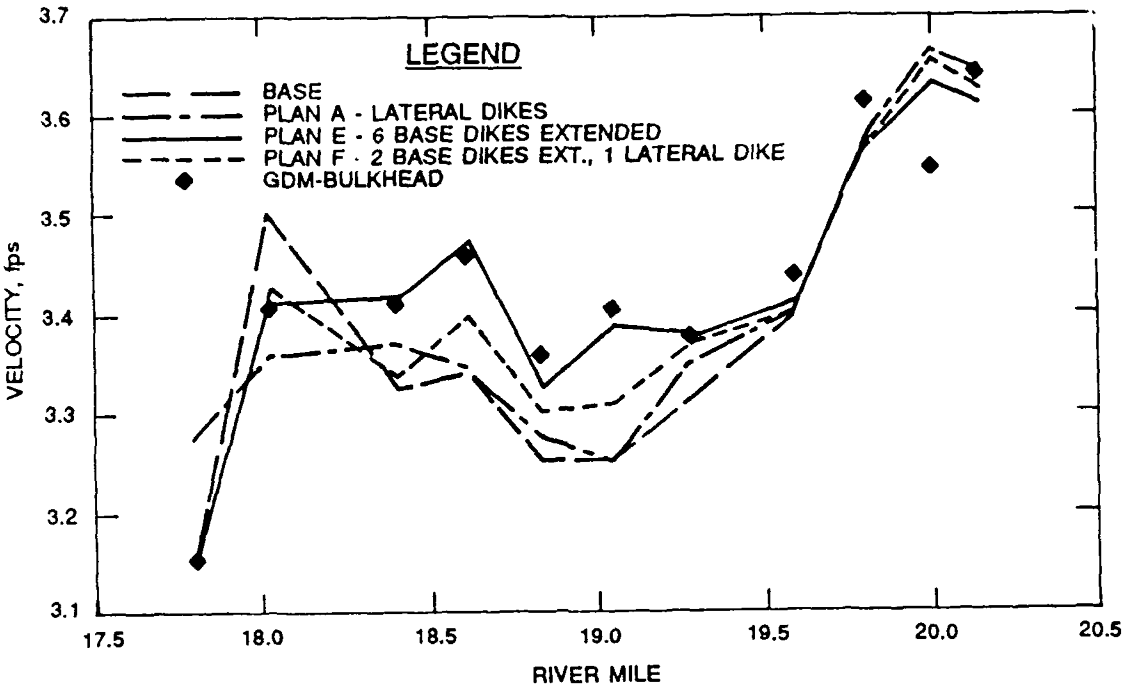

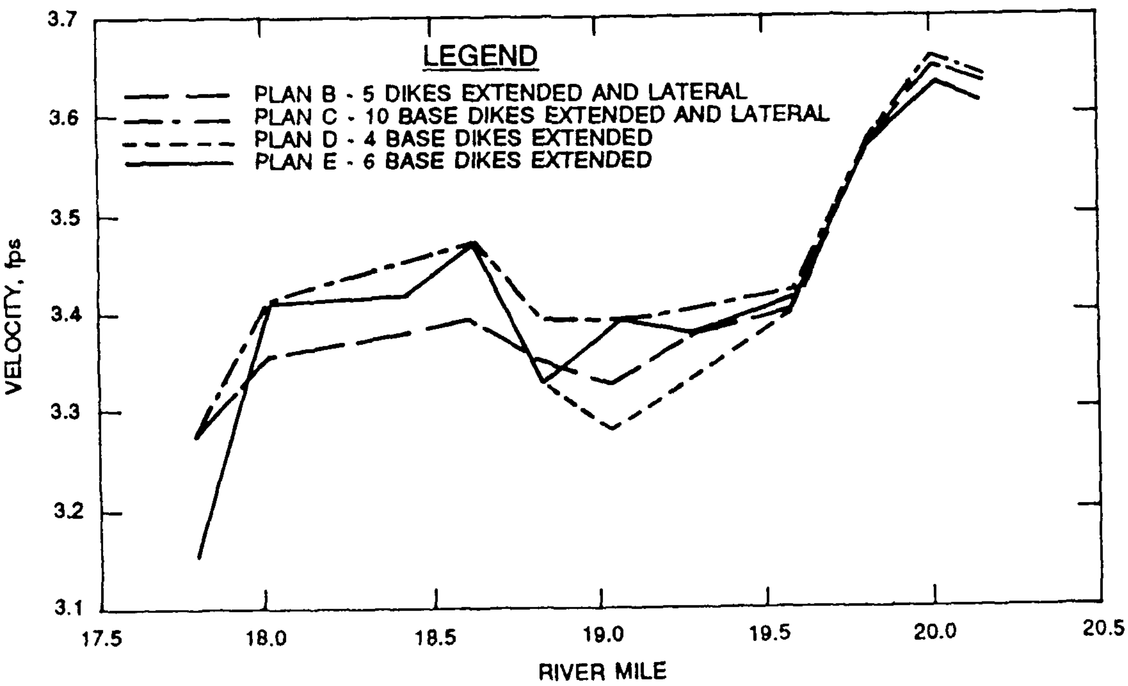

Figure 11. Weighted average velocity comparisons

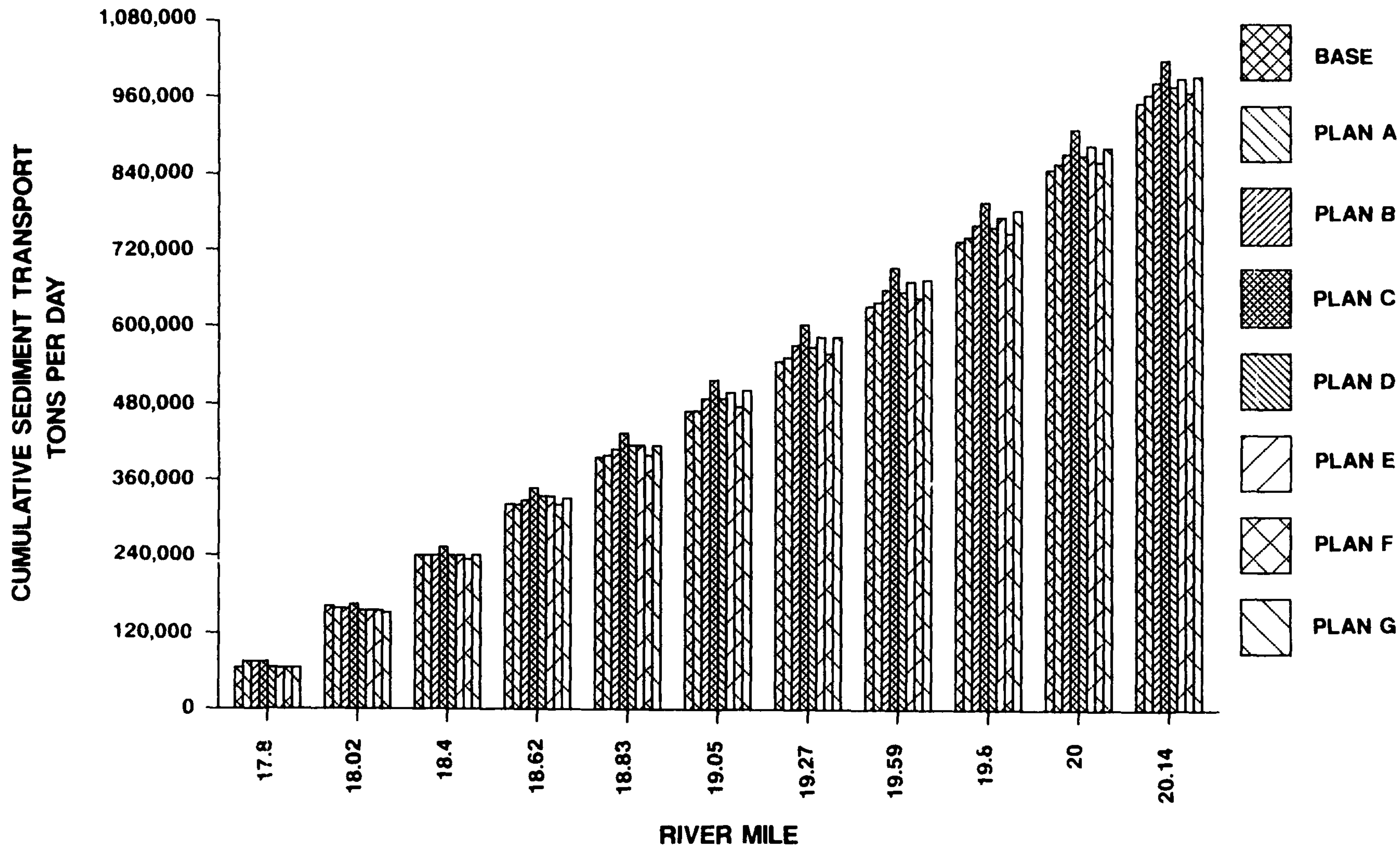

Figure 12. Sediment transport capacity comparisons

APPENDIX A: THE TABS-2 SYSTEM

1. TABS-2 is a collection of generalized computer programs and utility codes integrated into a numerical modeling system for studying two-dimensional hydrodynamics, sedimentation, and transport problems in rivers, reservoirs, bays, and estuaries. A schematic representation of the system is shown in Figure A1. It can be used either as a stand-alone solution technique or as a step in the hybrid modeling approach. The basic concept is to calculate water-surface elevations, current patterns, sediment erosion, transport and deposition, the resulting bed surface elevations, and the feedback to hydraulics. Existing and proposed geometry can be analyzed to determine the impact on sedimentation of project designs and to determine the impact of project designs on salinity and on the stream system. The system is described in detail by Thomas and McAnally (1985).

2. The three basic components of the system are as follows:

   a. "A Two-Dimensional Model for Free Surface Flows," RMA-2V.

   b. "Sediment Transport in Unsteady 2-Dimensional Flows, Horizontal Plane," STUDH.

   c. "Two-Dimensional Finite Element Program for Water Quality," RMA-4.

3. RMA-2V is a finite element solution of the Reynolds form of the Navier-Stokes equations for turbulent flows. Friction is calculated with Manning's equation and eddy viscosity coefficients are used to define the turbulent losses. A velocity form of the basic equation is used with side boundaries treated as either slip or static. The model automatically recognizes dry elements and corrects the mesh accordingly. Boundary conditions may be water-surface elevations, velocities, or discharges and may occur inside the mesh as well as along the edges.

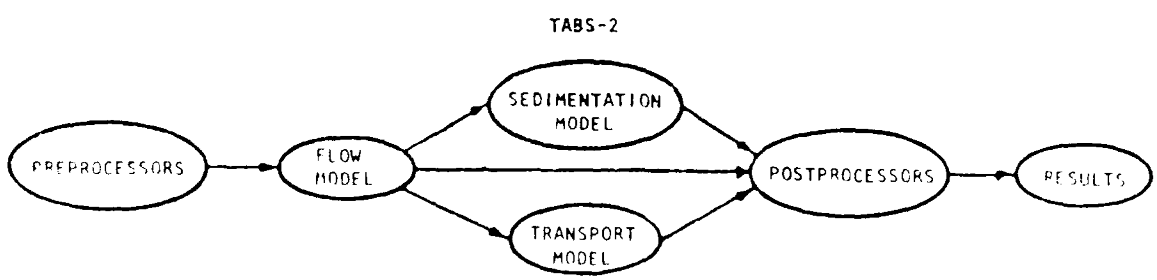

Figure A1. TABS-2 schematic

4. The sedimentation model, STUDH, solves the convection-diffusion equation with bed source terms. These terms are structured for either sand or cohesive sediments. The Ackers-White (1973) procedure is used to calculate a sediment transport potential for the sands from which the actual transport is calculated based on availability. Clay erosion is based on work by Partheniades (1962) and Ariathurai and the deposition of clay utilizes Krone's equations (Ariathurai, MacArthur, and Krone 1977). Deposited material forms layers, as shown in Figure A2, and bookkeeping allows up to 10 layers at each node for maintaining separate material types, deposit thickness, and age. The code uses the same mesh as RMA-2V.

5. Salinity calculations, RMA-4, are made with a form of the convective-diffusion equation which has general source-sink terms. Up to seven conservative substances or substances requiring a decay term can be routed. The code uses the same mesh as RMA-2V.

6. Each of these generalized computer codes can be used as a standalone program, but to facilitate the preparation of input data and to aid in analyzing results, a family of utility programs was developed for the following purposes:

- a. Digitizing
- b. Mesh generation
- c. Spatial data management
- d. Graphical output
- e. Output analysis
- f. File management
- g. Interfaces
- h. Job control language

Finite Element Modeling

7. The TABS-2 numerical models used in this effort employ the finite element method to solve the governing equations. To help those who are unfamiliar with the method to better understand this report, a brief description of the method is given here.

8. The finite element method approximates a solution to equations by dividing the area of interest into smaller subareas, which are called elements. The dependent variables (e.g., water-surface elevations and sediment

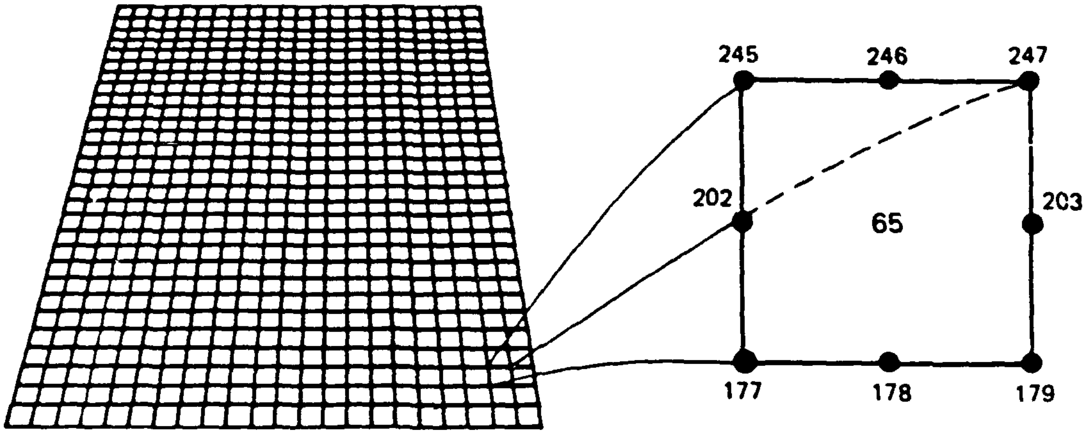

a. Eight nodes define each element

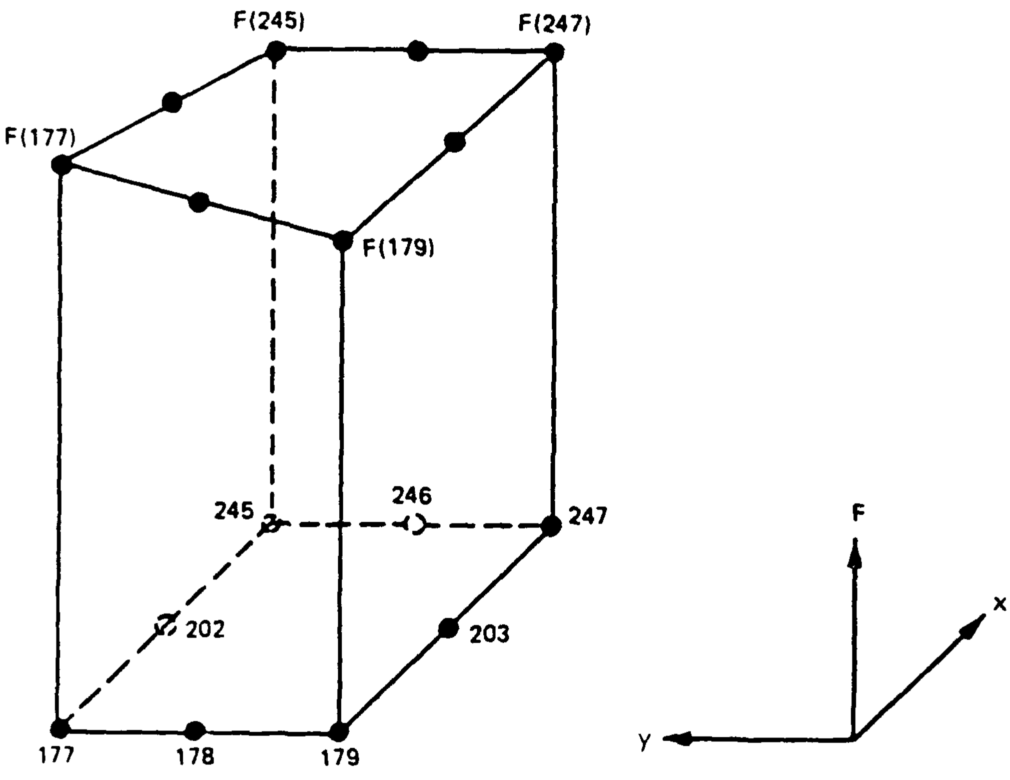

b. Linear interpolation function

Figure A2. Two-dimensional finite element mesh concentrations) are approximated over each element by continuous functions which interpolate in terms of unknown point (node) values of the variables. An error, defined as the deviation of the approximation solution from the correct solution, is minimized. Then, when boundary conditions are imposed, a set of solvable simultaneous equations is created. The solution is continuous over the area of interest.

9. In one-dimensional problems, elements are line segments. In two-dimensional problems, the elements are polygons, usually either triangles or quadrilaterals. Nodes are located on the edges of elements and occasionally inside the elements. The interpolating functions may be linear or higher order polynomials. Figure A2 illustrates a quadrilateral element with eight nodes and a linear solution surface where F is the interpolating function.

10. Most water resource applications of the finite element method use the Galerkin method of weighted residuals to minimize error. In this method the residual, the total error between the approximate and correct solutions, is weighted by a function that is identical with the interpolating function and then minimized. Minimization results in a set of simultaneous equations in terms of nodal values of the dependent variable (e.g. water-surface elevations or sediment concentration). The time portion of time-dependent problems can be solved by the finite element method, but it is generally more efficient to express derivatives with respect to time in finite difference form.

The Hydrodynamic Model, RMA-2V

Applications

11. This program is designed for far-field problems in which vertical accelerations are negligible and the velocity vectors at a node generally point in the same directions over the entire depth of the water column at any instant of time. It expects a homogeneous fluid with a free surface. Both steady and unsteady state problems can be analyzed. A surface wind stress can be imposed.

12. The program has been applied to calculate flow distribution around islands; flow at bridges having one or more relief openings, in contracting and expanding reaches, into and out of off-channel hydropower plants, at river junctions, and into and out of pumping plant channels; and general flow patterns in rivers, reservoirs, and estuaries.

Limitations

13. This program is not designed for near-field problems where flow-structure interactions (such as vortices, vibrations, or vertical accelerations) are of interest. Areas of vertically stratified flow are beyond this program's capability unless it is used in a hybrid modeling approach. It is two-dimensional in the horizontal plane, and zones where the bottom current is in a different direction from the surface current must be analyzed with considerable subjective judgment regarding long-term energy considerations. It is a free-surface calculation for subcritical flow problems.

Governing equations

14. The generalized computer program RMA-2V solves the depth-integrated equations of fluid mass and momentum conservation in two horizontal directions. The form of the solved equations is

$$h \frac{\partial u}{\partial t} + hu \frac{\partial u}{\partial x} + hv \frac{\partial u}{\partial y} - \frac{h}{\rho} \left(\varepsilon_{xx} \frac{\partial^2 u}{\partial x^2} + \varepsilon_{xy} \frac{\partial^2 u}{\partial y^2} \right) + gh \left(\frac{\partial a}{\partial x} + \frac{\partial h}{\partial x} \right)$$

$$+ \frac{gun^2}{\left(1.486h^{1/6}\right)^2} \left(u^2 + v^2 \right)^{1/2} - \zeta V_a^2 \cos \psi - 2h\omega v \sin \phi = 0 \qquad \text{(A1)}$$

$$h \frac{\partial v}{\partial t} + hv \frac{\partial v}{\partial x} + hv \frac{\partial v}{\partial y} - \frac{h}{\rho} \left(\varepsilon_{yx} \frac{\partial^2 v}{\partial x^2} + \varepsilon_{yy} \frac{\partial^2 v}{\partial y^2} \right) + gh \left(\frac{\partial a}{\partial y} + \frac{\partial h}{\partial y} \right)$$

$$+ \frac{gvn^2}{\left(1.486h^{1/6}\right)^2} \left(u^2 + v^2 \right)^{1/2} - \zeta V_a^2 \sin \psi + 2\omega hu \sin \phi = 0 \qquad \text{(A2)}$$

$$\frac{\partial h}{\partial t} + h \left(\frac{\partial u}{\partial x} + \frac{\partial v}{\partial y} \right) + u \frac{\partial h}{\partial x} + v \frac{\partial h}{\partial y} = 0 \qquad \text{(A3)}$$

where

h = depth

u,v = velocities in the Cartesian directions

x,y,t = Cartesian coordinates and time

ρ = density

ε = eddy viscosity coefficient, for xx = normal direction on x-axis surface; yy = normal direction on y-axis surface; xy and yx = shear direction on each surface

g = acceleration due to gravity

a = elevation of bottom

n = Manning's n value

1.486 = conversion from SI (metric) to non-SI units

ζ = empirical wind shear coefficient

V_a = wind speed

ψ = wind direction

ω = rate of earth's angular rotation

ϕ = local latitude

15. Equations A1, A2, and A3 are solved by the finite element method using Galerkin weighted residuals. The elements may be either quadrilaterals or triangles and may have curved (parabolic) sides. The shape functions are quadratic for flow and linear for depth. Integration in space is performed by Gaussian integration. Derivatives in time are replaced by a nonlinear finite difference approximation. Variables are assumed to vary over each time interval in the form

$$f(t) = f(0) + at + bt^c \qquad t_0 \leq t < t \tag{A4}$$

which is differentiated with respect to time, and cast in finite difference form. Letters a , b , and c are constants. It has been found by experiment that the best value for c is 1.5 (Norton and King 1977).

16. The solution is fully implicit and the set of simultaneous equations is solved by Newton-Raphson iteration. The computer code executes the solution by means of a front-type solver that assembles a portion of the matrix and solves it before assembling the next portion of the matrix. The front solver's efficiency is largely independent of bandwidth and thus does not require as much care in formation of the computational mesh as do traditional solvers.

17. The code RMA-2V is based on the earlier version RMA-2 (Norton and King 1977) but differs from it in several ways. It is formulated in terms of velocity (v) instead of unit discharge (vh), which improves some aspects of the code's behavior; it permits drying and wetting of areas within the grid;

and it permits specification of turbulent exchange coefficients in directions other than along the x- and z-axes. For a more complete description, see Appendix F of Thomas and McAnally (1985).

The Sediment Transport Model, STUDH

Applications

18. STUDH can be applied to clay and/or sand bed sediments where flow velocities can be considered two-dimensional (i.e., the speed and direction can be satisfactorily represented as a depth-averaged velocity). It is useful for both deposition and erosion studies and, to a limited extent, for stream width studies. The program treats two categories of sediment: noncohesive, which is referred to as sand here, and cohesive, which is referred to as clay.

Limitations

19. Both clay and sand may be analyzed, but the model considers a single, effective grain size for each and treats each separately. Fall velocity must be prescribed along with the water-surface elevations, x-velocity, y-velocity, diffusion coefficients, bed density, critical shear stresses for erosion, erosion rate constants, and critical shear stress for deposition.

20. Many applications cannot use long simulation periods because of their computation cost. Study areas should be made as small as possible to avoid an excessive number of elements when dynamic runs are contemplated yet must be large enough to permit proper posing of boundary conditions. The same computation time interval must be satisfactory for both the transverse and longitudinal flow directions.

21. The program does not compute water-surface elevations or velocities; therefore, these data must be provided. For complicated geometries, the numerical model for hydrodynamic computations, RMA-2V, is used.

Governing equations

22. The generalized computer program STUDH solves the depth-integrated convection-dispersion equation in two horizontal dimensions for a single sediment constituent. For a more complete description, see Appendix G of Thomas and McAnally (1985). The form of the solved equation is

$$\frac{\partial C}{\partial t} + u\frac{\partial C}{\partial x} + v\frac{\partial C}{\partial y} = \frac{\partial}{\partial x}\left(D_x \frac{\partial C}{\partial x}\right) + \frac{\partial}{\partial y}\left(D_y \frac{\partial C}{\partial y}\right) + \alpha_1 C + \alpha_2 = 0 \qquad \text{(A5)}$$

where

C = concentration of sediment

u = depth-integrated velocity in x-direction

v = depth-integrated velocity in y-direction

D_x = dispersion coefficient in x-direction

D_y = dispersion coefficient in y-direction

α_1 = coefficient of concentration-dependent source/sink term

α_2 = coefficient of source/sink term

23. The source/sink terms in Equation A5 are computed in routines that treat the interaction of the flow and the bed. Separate sections of the code handle computations for clay bed and sand bed problems.

Sand transport

24. The source/sink terms are evaluated by first computing a potential sand transport capacity for the specified flow conditions, comparing that capacity with the amount of sand actually being transported, and then eroding from or depositing to the bed at a rate that would approach the equilibrium value after sufficient elapsed time.

25. The potential sand transport capacity in the model is computed by the method of Ackers and White (1973), which uses a transport power (work rate) approach. It has been shown to provide superior results for transport under steady-flow conditions (White, Milli, and Crabbe 1975) and for combined waves and currents (Swart 1976). Flume tests at the US Army Engineer Waterways Experiment Station have shown that the concept is valid for transport by estuarine currents.

26. The total load transport function of Ackers and White is based upon a dimensionless grain size

$$D_{gr} = D \left[\frac{g(s - 1)}{\nu^2} \right]^{1/3} \qquad \text{(A6)}$$

where

D = sediment particle diameter

s = specific gravity of the sediment

ν = kinematic viscosity of the fluid

and a sediment mobility parameter

$$F_{gr} = \left[\frac{\tau^{n'} \tau'^{(1-n')}}{\rho g D(s - 1)} \right]^{1/2} \tag{A7}$$

where

τ = total boundary shear stress

n' = a coefficient expressing the relative importance of bed-load and suspended-load transport, given in Equation A9

τ' = boundary surface shear stress

The surface shear stress is that part of the total shear stress which is due to the rough surface of the bed only, i.e., not including that part due to bed forms and geometry. It therefore corresponds to that shear stress that the flow would exert on a plane bed.

27. The total sediment transport is expressed as an effective concentration

$$G_P = C\left(\frac{F_{gr}}{A} - 1\right)^m \frac{sD}{h} \left(\frac{\rho}{\tau} U\right)^{n'} \tag{A8}$$

where U is the average flow speed, and for $1 < D_{gr} \leq 60$

$$n' = 1.00 - 0.56 \log D_{gr} \tag{A9}$$

$$A = \frac{0.23}{\sqrt{D_{gr}}} + 0.14 \tag{A10}$$

$$\log C = 2.86 \log D_{gr} - (\log D_{gr})^2 - 3.53 \tag{A11}$$

$$m = \frac{9.66}{D_{gr}} + 1.34 \tag{A12}$$

For $D_{gr} < 60$

$$n' = 0.00 \tag{A13}$$

$$A = 0.17 \tag{A14}$$

$$C = 0.025 \tag{A15}$$

$$m = 1.5 \tag{A16}$$

28. Equations A6-A16 result in a potential sediment concentration G_p. This value is the depth-averaged concentration of sediment that will occur if an equilibrium transport rate is reached with a nonlimited supply of sediment. The rate of sediment deposition (or erosion) is then computed as

$$R = \frac{G_p - C}{t_c} \tag{A17}$$

where

C = present sediment concentration

t_c = time constant

For deposition, the time constant is

$$t_c = \text{larger of} \left\{ \begin{array}{l} \Delta t \\ \text{or} \\ \dfrac{C_d h}{V_s} \end{array} \right. \tag{A18}$$

and for erosion it is

$$t_c = \text{larger of} \left\{ \begin{array}{l} \Delta t \\ \text{or} \\ \dfrac{C_e h}{U} \end{array} \right. \tag{A19}$$

where

Δt = computational time-step

C_d = response time coefficient for deposition

V_s = sediment settling velocity

C_e = response time coefficient for erosion

The sand bed has a specified initial thickness which limits the amount of erosion to that thickness.

Cohesive sediments transport

29. Cohesive sediments (usually clays and some silts) are considered to be depositional if the bed shear stress exerted by the flow is less than a critical value τ_d . When that value occurs, the deposition rate is given by Krone's (1962) equation

$$S = \begin{cases} -\dfrac{2V_s}{h} C \left(1 - \dfrac{\tau}{\tau_d}\right) \quad \text{for} \quad C < C_c & \text{(A20)} \\ \\ -\dfrac{2V_s}{hC_c^{4/3}} C^{5/3} \left(1 - \dfrac{\tau}{\tau_d}\right) \quad \text{for} \quad C > C_c & \text{(A21)} \end{cases}$$

where

S = source term

V_s = fall velocity of a sediment particle

h = flow depth

C = sediment concentration in water column

τ = bed shear stress

τ_d = critical shear stress for deposition

C_c = critical concentration = 300 mg/ℓ

30. If the bed shear stress is greater than the critical value for particle erosion τ_e , material is removed from the bed. The source term is then computed by Ariathurai's (Ariathurai, MacArthur, and Krone 1977) adaptation of Partheniades' (1962) findings:

$$S = \frac{P}{h}\left(\frac{\tau}{\tau_e} - 1\right) \quad \text{for} \quad \tau > \tau_e \tag{A22}$$

where P is the erosion rate constant, unless the shear stress is also greater than the critical value for mass erosion. When this value is exceeded, mass failure of a sediment layer occurs and

$$S = \frac{T_L P_L}{h\Delta t} \quad \text{for } \tau > \tau_s \tag{A23}$$

where

T_L = thickness of the failed layer

P_L = density of the failed layer

Δt = time interval over which failure occurs

τ_s = bulk shear strength of the layer

31. The cohesive sediment bed consists of 1 to 10 layers, each with a distinct density and erosion resistance. The layers consolidate with overburden and time.

Bed shear stress

32. Bed shear stresses are calculated from the flow speed according to one of four optional equations: the smooth-wall log velocity profile or Manning equation for flows alone; and a smooth bed or rippled bed equation for combined currents and wind waves. Shear stresses are calculated using the shear velocity concept where

$$\tau_b = \rho u_*^2 \tag{A24}$$

where

τ_b = bed shear stress

u_* = shear velocity

and the shear velocity is calculated by one of four methods:

a. Smooth-wall log velocity profiles

$$\frac{\bar{u}}{u_*} = 5.75 \log \left(3.32 \frac{u_* h}{\nu}\right) \tag{A25}$$

which is applicable to the lower 15 percent of the boundary layer when

$$\frac{u_* h}{\nu} > 30$$

where u is the mean flow velocity (resultant of u and v components)

b. The Manning shear stress equation

$$u_* = \frac{(\bar{u}n)\sqrt{g}}{CME\ (h)^{1/6}} \tag{A26}$$

where CME is a coefficient of 1 for SI (metric) units and 1.486 for non-SI units of measurement.

c. A Jonsson-type equation for surface shear stress (plane beds) caused by waves and currents

$$u_* = \sqrt{\frac{1}{2}\left(\frac{f_w u_{om} + f_c \bar{u}}{u_{om} + \bar{u}}\right)\left(\bar{u} + u_{om}\right)^2} \tag{A27}$$

where

f_w = shear stress coefficient for waves

u_{om} = maximum orbital velocity of waves

f_c = shear stress coefficient for currents

d. A Bijker-type equation for total shear stress caused by waves and current

$$u_* = \sqrt{\frac{1}{2} f_c \bar{u}^2 + \frac{1}{4} f_w u_{om}^2} \tag{A28}$$

Solution method

33. Equation A5 is solved by the finite element method using Galerkin weighted residuals. Like RMA-2V, which uses the same general solution technique, elements are quadrilateral and may have parabolic sides. Shape functions are quadratic. Integration in space is Gaussian. Time-stepping is performed by a Crank-Nicholson approach with a weighting factor (θ) of 0.66. A front-type solver similar to that in RMA-2V is used to solve the simultaneous equations.

REFERENCES

Ackers, P., and White, W. R. 1973 (Nov). "Sediment Transport: New Approach and Analysis," Journal, Hydraulics Division, American Society of Civil Engineers, No. HY-11.

Ariathurai, R., MacArthur, R. D., and Krone, R. C. 1977 (Oct). "Mathematical Model of Estuarial Sediment Transport," Technical Report D-77-12, US Army Engineer Waterways Experiment Station, Vicksburg, MS.

Krone, R. B. 1962. "Flume Studies of Transport of Sediment in Estuarial Shoaling Processes," Final Report, Hydraulics Engineering Research Laboratory, University of California, Berkeley, CA.

Norton, W. R., and King, I. P. 1977 (Feb). "Operating Instructions for the Computer Program RMA-2V," Resource Management Associates, Lafayette, CA.

Partheniades, E. 1962. "A Study of Erosion and Deposition of Cohesive Soils in Salt Water," Ph.D. Dissertation, University of California, Berkeley, CA.

Swart, D. H. 1976 (Sep). "Coastal Sediment Transport, Computation of Longshore Transport," R968, Part 1, Delft Hydraulics Laboratory, The Netherlands.

Thomas, W. A., and McAnally, W. H., Jr. 1985 (Aug). "User's Manual for the Generalized Computer Program System; Open-Channel Flow and Sedimentation, TABS-2, Main Text and Appendices A through O," Instruction Report HL-85-1, US Army Engineer Waterways Experiment Station, Vicksburg, MS.

White, W. R., Milli, H., and Crabbe, A. D. 1975. "Sediment Transport Theories: An Appraisal of Available Methods," Report Int 119, Vols 1 and 2, Hydraulics Research Station, Wallingford, England.